patient-oriented and epidemiological research

A physiologically based in silico kinetic model predicting plasma cholesterol concentrations in humans[S]

Niek C. A. van de Pas,*,†,§ Ruud A. Woutersen,*,†,§ Ben van Ommen,* Ivonne M. C. M. Rietjens,†,§ and Albert A. de Graaf[1],*

The Netherlands Organization for Applied Scientific Research (TNO),* 3700 AJ Zeist, The Netherlands; Division of Toxicology,† Wageningen University, 6703 HE Wageningen, The Netherlands; and TNO/WUR Centre for Innovative Toxicology,§ 6703 HE Wageningen, The Netherlands

Abstract **Increased plasma cholesterol concentration is associated with increased risk of cardiovascular disease. This study describes the development, validation, and analysis of a physiologically based kinetic (PBK) model for the prediction of plasma cholesterol concentrations in humans. This model was directly adapted from a PBK model for mice by incorporation of the reaction catalyzed by cholesterol ester transfer protein and contained 21 biochemical reactions and eight different cholesterol pools. The model was calibrated using published data for humans and validated by comparing model predictions on plasma cholesterol levels of subjects with 10 different genetic mutations (including familial hypercholesterolemia and Smith-Lemli-Opitz syndrome) with experimental data. Average model predictions on total cholesterol were accurate within 36% of the experimental data, which was within the experimental margin. Sensitivity analysis of the model indicated that the HDL cholesterol (HDL-C) concentration was mainly dependent on hepatic transport of cholesterol to HDL, cholesterol ester transfer from HDL to non-HDL, and hepatic uptake of cholesterol from non-HDL-C. Thus, the presented PBK model is a valid tool to predict the effect of genetic mutations on cholesterol concentrations, opening the way for future studies on the effect of different drugs on cholesterol levels in various subpopulations in silico.**—van de Pas, N. C. A., R. A. Woutersen, B. van Ommen, I. M. C. M. Rietjens, and A. A. de Graaf. **A physiologically based in silico kinetic model predicting plasma cholesterol concentrations in humans.** ***J. Lipid Res.*** **2012. 53: 2734–2746.**

Supplementary key words plasma cholesterol • PBK modeling • mutations • LDL cholesterol • HDL cholesterol

In silico modeling has proven to be a useful tool in biology because it allows the study of interspecies variation and regulation of homeostasis and allows the integration of information from various sources (1–3). There are several modeling efforts on cholesterol (4–7), an important biomarker for the risk for cardiovascular events (8–10). Most of these cholesterol modeling studies present models that focus on LDL cholesterol (LDL-C) metabolism in plasma (4–6) or on cellular cholesterol metabolism (7). These models do not represent all relevant components of whole body cholesterol homeostasis because they lack reactions such as cholesterol absorption and biosynthesis in organs, which are the reactions targeted by important cholesterol-lowering drugs, such as statins. This implies that the models cannot fully explain how relevant plasma cholesterol-associated biomarkers are influenced by these drug interventions.

We have, therefore, developed an in silico physiologically based kinetic (PBK) model for plasma cholesterol in the mouse that includes all relevant reactions and that correctly predicts the plasma cholesterol levels of a large variety of mouse strains with gene knockouts related to cholesterol metabolism (11). The model, of which the structure is given in **Fig. 1**, is able to predict HDL cholesterol (HDL-C), non-HDL cholesterol (non-HDL-C), and total plasma cholesterol (TC) concentrations (12) as well as the intra-organ pools representing hepatic free cholesterol (Liv-FC), peripheral cholesterol (Per-C), intestinal cholesterol ester (Int-CE), hepatic cholesterol ester (Liv-CE), and intestinal free cholesterol (Int-FC) in the mouse. A similar model for humans will be of considerable value in predicting effects of drugs and genetic variations on plasma cholesterol concentrations. Therefore, the aim of this work is to adapt our model to a human version.

Turnover of cholesterol in humans is quantitatively and qualitatively different from that in mice (13). Qualitative difference resides mainly in the protein cholesteryl ester

Manuscript received 4 September 2012 and in revised form 28 September 2012.
Published, JLR Papers in Press, September 29, 2012
DOI 10.1194/jlr.M031930

Abbreviations: C, cholesterol (sum of FC and CE); CE, cholesterol ester; CETP, cholesterol ester transfer protein; FC, free cholesterol; FH, familial hypercholesterolemia; GWAS, genome-wide association study; PBK, physiologically based kinetic; SC, sensitivity coefficient; SLOS, Smith-Lemli-Opitz syndrome; TC, total plasma cholesterol (sum of HDL-C and non-HDL-C).

[1]To whom correspondence should be addressed.
e-mail: albert.degraaf@tno.nl

[S] The online version of this article (available at http://www.jlr.org) contains supplementary data in the form of supplementary data, tables and references.

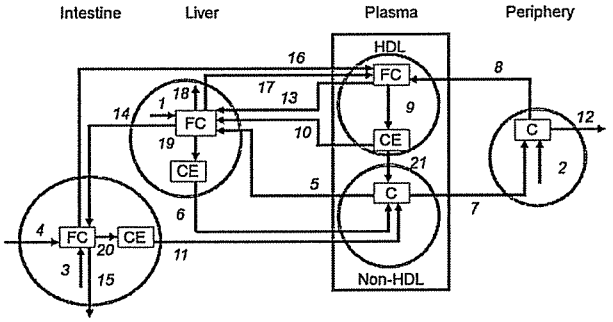

Fig. 1. Conceptual model for pathways determining cholesterol plasma levels used as a basis to set up the in silico model of the present study. Process numbers stand for: 1, hepatic cholesterol synthesis; 2, peripheral cholesterol synthesis; 3, intestinal cholesterol synthesis; 4, dietary cholesterol intake; 5, hepatic uptake of cholesterol from LDL; 6, VLDL-C secretion; 7, peripheral uptake of cholesterol from LDL; 8, peripheral cholesterol transport to HDL; 9, HDL-associated cholesterol esterification; 10, hepatic HDL-CE uptake; 11, intestinal chylomicron cholesterol secretion; 12, peripheral cholesterol loss; 13, hepatic HDL-FC uptake; 14, biliary cholesterol excretion; 15, fecal cholesterol excretion; 16, intestinal cholesterol transport to HDL; 17, hepatic cholesterol transport to HDL; 18, hepatic cholesterol catabolism; 19, hepatic cholesterol esterification; 20, intestinal cholesterol esterification; and 21, CE transfer from HDL to LDL. Based on Ref. 11.

transfer protein (CETP), which is present in humans and other primates but absent in mice and other rodents (14). CETP transfers cholesterol ester (CE) from HDL to LDL, thereby greatly influencing the distribution of cholesterol over the different plasma fractions (HDL-C and non-HDL-C). The importance of the CETP gene is illustrated by the observation that a specific mutation in this gene causes a 10% increase in HDL-C levels (15). The pharmaceutical industry has recognized the importance of this gene, resulting in the development of CETP modulators that aim to increase the concentrations of HDL-C (16–18).

Apart from this qualitative difference, there are many quantitative differences between mouse and human with respect to parameters that influence cholesterol turnover, such as dietary intake, transport and synthesis rates of cholesterol, and organ sizes (13, 19). Some of these differences persist even after correcting for differences in body mass. For example, according to Dietschy and Turley (13), the amount of cholesterol absorbed from the diet per kilogram of body mass is 30 mg cholesterol/kg body mass/day in the mouse, compared with only 5 mg cholesterol/kg body mass/day for human. Consequently, translationally modifying the available mouse model for human subjects is not straightforward. This study describes this translation, as well as a validation of the resulting model, by simulating human mutations and comparing the model predictions on HDL-C and non-HDL-C in plasma concentrations with experimental data reported in literature.

MATERIALS AND METHODS

The development of the in silico model was subdivided into the following steps: development of a conceptual model (model structure), mathematical formulation of the model, model calibration, and model validation. After development, a sensitivity analysis was performed to obtain more insight into the factors that determine plasma cholesterol concentrations.

Conceptual model development

The conceptual model for the human PBK model was modified from the conceptual model for the mouse (11). Briefly, the mouse model was constructed as follows: relevant knockout mouse models were screened for altered plasma cholesterol levels compared with the levels in the wild-type mouse. If the alteration was more than 2-fold (up or down) compared with the wild-type, the corresponding gene was marked as a key gene. Based on the function of a subset of 12 of these key genes that code for metabolic enzymes producing or consuming cholesterol and transport proteins transporting cholesterol, metabolic and transport reactions were included in the mouse conceptual model (11). The conceptual model for the human was developed from the mouse model by adding human-specific features (see Results). In view of the sparsity of data available to calibrate and validate the model, the number of pools and fluxes in the model was kept to a minimum to avoid overparametrization. As a consequence, FC and CE pools were not distinguished in plasma non-HDL and in the periphery. Also, in the intestine, luminal and enterocytic pools were not distinguished (i.e., the aggregate pools were used).

Mathematical model formulation

As the second step in the model development, the conceptual model was converted to mathematical equations. Similar to the mouse model, the human model was formulated as a set of differential equations, each describing the time behavior of one of the cholesterol pools in the conceptual model as a function of the reaction rates.

Equations were slightly altered compared with the mouse model: for the human model, reaction rates were expressed as mmol/man/day, where "man" refers to a standard human, leading to more simple equations (12). For practical reasons, reaction rates (expressed by v_i) were numbered according to the numbering in Fig. 1. All symbols of variables and parameters that were used to define the model are given in **Table 1**. The differential equations, one for each cholesterol pool in the model, are given in **Table 2** (Eq. 1–8). Eq. 1, for example, can be interpreted as follows: the change in time of the concentration of hepatic free cholesterol is determined by the balance of the rates of the reactions producing (v_1, v_5, v_{10}, v_{13}) and consuming (v_{14}, v_{17}, v_{18}, v_{19}) hepatic free cholesterol.

In a kinetic model, the reaction rates are calculated using kinetic equations that express the reaction rate as a function of concentrations and kinetic parameters. Most reactions in our model represent a set of lumped enzymatic and/or transport reactions. Often, such a composite reaction can be conveniently represented by a kinetic equation that contains apparent rate constants and apparent K_M values. A general solution is to use Michaelis-Menten kinetics as a prototype kinetic expression for biological reactions. In the present approach, to keep the number of parameters as limited as possible, it was assumed that the reactions operate in the linear part of a Michaelis-Menten kinetic curve (substrate concentration much lower than the apparent K_M) or in the saturated part (substrate concentration much higher than the apparent K_M). At low substrate concentrations, Michaelis-Menten kinetics effectively reduce to first-order kinetics (Eq. 9; Table 2). At high substrate concentrations, Michaelis-Menten kinetics reduce to zero-order kinetics (i.e., the reaction becomes independent of the substrate concentration) (Eq. 10; Table 2).

TABLE 1. List of symbols and parameters used

Symbol	Description	Unit
V_i	volume of compartment i with i = Liv, Pla, Per, and Int for liver, plasma, periphery, and intestine	L/man
v_i	reaction rate of reaction i	mmol/(man·day)
v_i^{ss}	steady state reaction rate of reaction i	mmol/(man·day)
$[C]_i$	tissue or plasma concentration of pool i, with i = Liv-FC, HDL-FC, HDL-CE, non-HDL-C, Per-C, Int-FC, Liv-CE, and Int-CE for liver free cholesterol, HDL free cholesterol, HDL cholesterol ester, non-HDL cholesterol, peripheral cholesterol, intestinal free cholesterol, liver cholesterol ester, and intestinal cholesterol ester	mmol/l
$[C]_i^{ss}$	steady-state concentration of pool i	mmol/l
k_i^z	zero-order rate constant of reaction i	mmol/(liter·day)
k_i^f	first-order rate constant of reaction i	liter/day
k_i^s	second-order rate constant of reaction i	liter/(mmol·day)
$k_i^{mut,j}$	j^{th}-order rate constant of reaction i in a human carrying a mutation that affects reaction i	
$k_i^{*,k}$	k^{th}-order reaction rate constant of reaction i that has been altered compared with the normal values	
$[C]_i^{*,ss}$	steady-state concentration of pool I, in case the reaction rate constant of reaction i that has been altered compared with the normal values	mmol/l
t	time	day
f_{mut}	rate constant modification factor	[-]

Reaction 21, catalyzed by CETP, was assumed to have kinetics different from the other reactions. CETP transfers CE from HDL to LDL and requires the binding of both a donor (HDL) and acceptor particle (non-HDL) to exchange cholesterol (20,21). Therefore, the rate of this reaction was dependent on HDL-CE and non-HDL-CE. It was assumed that the reaction rate was linear with respect to both concentrations as given by Eq. 11 (Table 2).

The kinetic formats of reactions 1–20 were obtained from the previously defined mouse model. Instead of developing one optimal model, the mouse model consists of a set (ensemble) of eight submodels, each having a different combination of first- and zero-order kinetics for the various reactions. The model prediction is calculated as the average of the predictions of the submodels. These eight submodels have been selected from a larger set of 65,536 alternative submodels. Each of the suitable submodels has been selected on the basis of a correct prediction of a higher or lower plasma cholesterol level of five knockout mouse strains compared with the wild-type controls (12). For the human situation, not enough data were available to apply an identical selection procedure. Therefore, it was decided to use the kinetic formats of the reactions 1–20 in the eight submodels for the mouse also for the corresponding reactions in the human model. Thus, the eight mouse submodels were converted to eight human submodels, retaining the kinetic orders of reactions 1–20 and adding reaction 21. As in the mouse model, the human model prediction was defined as the average of the predictions of the resulting eight submodels. The predicted TC concentration was calculated as the sum of all three types of plasma cholesterol (non-HDL-C, HDL free cholesterol [HDL-FC], and HDL-CE), whereas the predicted HDL-C concentration was calculated as the sum of HDL-FC and HDL-CE.

Model calibration

The model was calibrated by assigning values to the kinetic parameters (k_i^z, k_i^f, and k_i^s). The values of the parameters were calculated from steady-state concentrations of cholesterol pools and reaction rates of the reactions obtained from literature. Literature data on reaction rates and pool sizes were taken from a wide range of experiments including cannulations, dietary surveys, and in vitro tests, as explained in detail below. Regarding reaction rates, we concentrated on data from experiments that had directly assessed rates that were attributable to a specific reaction in our model.

As usual in PBK modeling (3, 19), the model was developed for a standard human, for which we chose the 70 kg "reference man" as defined by the International Commission on Radiation Protection (19). Thus, data on 70 kg adult male subjects were taken as much as possible. In case the data were obtained from subjects with different body masses, reaction rates were normalized per unit of organ volume and multiplied by the organ mass of the reference man to obtain the reaction rate for the standard human.

If a specific submodel a rate was calculated for a first-order reaction, the corresponding rate constant was calculated using the pool sizes and steady-state reaction rates according to Eq. 12 (Table 2). In the case of a zero-order reaction, the corresponding rate constant was calculated according to Eq. 13 (Table 2). To calculate the rate constant of reaction 21, Eq. 14 was used (Table 2).

Model validation

To validate the model, the model was used to predict the plasma cholesterol concentrations of humans carrying genetic mutations, and these predictions were compared with experimental data obtained from literature. A genetic mutation was simulated by a model run with a case-specific set of parameters different from the normal situation, as follows. The rate constants for the reactions primarily affected by the given mutation were multiplied with a specific parameter (f_{mut}), according to Eq. 15, 16, or 17 (Table 2). This multiplication reflects the impact of the mutation on the reaction rate constant (i.e., fold reduction or increase). All other parameters were assumed to be unaffected by the given mutation. The values for f_{mut} for each individual mutation were defined based on literature data as described in the Results section.

TABLE 2. Equations used in model development (Eq. 1–11), model calibration (Eq. 12–14), for simulation of the effect of human mutations (Eq. 15–17), and sensitivity analysis (Eq. 18)

Differential Equations	
$\frac{d\left(V_{Liv}\cdot[C]_{Liv-FC}\right)}{dt} = v_1 + v_5 + v_{10} + v_{13} - v_{19} - v_{14} - v_{17} - v_{18}$	Eq. 1
$\frac{d\left(V_{Pla}\cdot[C]_{HDL-FC}\right)}{dt} = v_8 + v_{16} + v_{17} - v_9 - v_{13}$	Eq. 2
$\frac{d\left(V_{Pla}\cdot[C]_{HDL-CE}\right)}{dt} = v_9 - v_{10} - v_{21}$	Eq. 3
$\frac{d\left(V_{Pla}\cdot[C]_{non\ HDL-C}\right)}{dt} = v_6 + v_{11} - v_5 - v_7 + v_{21}$	Eq. 4
$\frac{d\left(V_{Per}\cdot[C]_{Per-C}\right)}{dt} = v_2 + v_7 - v_8 - v_{12}$	Eq. 5
$\frac{d\left(V_{Int}\cdot[C]_{Int-FC}\right)}{dt} = v_3 + v_4 + v_{14} - v_{20} - v_{16} - v_{15}$	Eq. 6
$\frac{d\left(V_{Liv}\cdot[C]_{Liv-CE}\right)}{dt} = v_{19} - v_6$	Eq. 7
$\frac{d\left(V_{Int}\cdot[C]_{Int-CE}\right)}{dt} = v_{20} - v_{11}$	Eq. 8
Rate equations	
$v_i = k_i^z \cdot V$ (zero-order kinetics)	Eq. 9
$v_i = k_i^f \cdot V \cdot [C]$ (first-order kinetics)	Eq. 10
$v_{21} = k_{21}^s \cdot [C]_{HDL-CE} \cdot [C]_{non\ HDL-C} \cdot V$ (second-order kinetics)	Eq. 11
Model calibration	
$k_i^z = v_i^{ss} / V$ (zero-order kinetics)	Eq. 12
$k_i^f = \frac{v_i^{ss}}{[C]_i^{ss}\cdot V}$ (first-order kinetics)	Eq. 13
$k_{21}^s = \frac{v_{21}^{ss}}{[C]_{HDL-CE}^{ss}\cdot[C]_{non\ HDL-C}^{ss}\cdot V}$ (second-order kinetics)	Eq. 14
Mutation simulation	
$k_i^{mut,z} = f_{mut}\cdot k_i^z$ (zero-order kinetics)	Eq. 15
$k_i^{mut,f} = f_{mut}\cdot k_i^f$ (first-order kinetics)	Eq. 16
$k_{21}^{mut,s} = f_{mut}\cdot k_{21}^s$ (second-order kinetics)	Eq. 17
Sensitivity analysis	
$SC_{ij} = \frac{[C]_j^{*,ss} - [C]_j^{ss}}{[C]_j^{ss}} \frac{k_i^k}{k_i^k - k_i^{*,k}}$	Eq. 18

Model predictions were derived as follows: the differential equations (Eq. 1–8) were solved by numerical integration with the normal concentrations as initial values. Integration was performed using routine *ode15s* as implemented in MATLAB version 7.5 (R2007b) with the appropriate parameter value(s) for each subject (normal or mutant). The simulation was performed until steady state of all cholesterol pools in the model was achieved. Model predictions were defined as these steady-state concentrations.

JOURNAL OF LIPID RESEARCH ASBMB

Sensitivity analysis

To identify which reactions had a large influence on the eight predicted cholesterol pools in the model, a sensitivity analysis was performed. Percent changes in reaction rates were related to percent changes in tissue and plasma cholesterol pools. One by one, each kinetic constant was increased by 1% (leaving all other kinetic constants unchanged), and the model was used to predict the effect of this increase on all eight cholesterol pools that figured in the model. This analysis includes the response of all reactions in the model to the change in this kinetic constant. The effect of the increase in parameter of rate i on pool j was expressed in a sensitivity coefficient (SC) as defined in Eq. 18. The SC of the model was defined as the average of the SCs calculated with the eight submodels.

RESULTS

Conceptual model development

Fig. 1 presents the conceptual model for human plasma cholesterol levels. The model contains eight pools and 21 reactions, such as hepatic cholesterol synthesis (reaction 1), biliary cholesterol excretion (reaction 14), fecal cholesterol excretion (reaction 15), and CETP (reaction 21).

Model development and calibration

The human PBK model was formulated as differential equations (Eq. 1–8; Table 2) and rate equations (Eq. 9–11; Table 2) based on the conceptual model given in Fig. 1. The model was calibrated using compartmental volumes, steady-state cholesterol concentrations, and rates of cholesterol-involving reactions derived from literature. A detailed description of how data were derived, transformed into the correct units, and scaled to the 70 kg "reference man" as defined by the International Commission on Radiation Protection (19) can be found in the supplementary material. Concerning plasma cholesterol, the total plasma cholesterol concentrations were 5.25 mM for TC and 1.19 mM for HDL-C as was obtained from an inventory of data from 8809 US adults (22). Plasma cholesterol not present in the HDL-C pool (4.03 mM) was considered to be present in the non-HDL-C pool. The total HDL-C concentration (HDL-C, 1.19 mM) consists of HDL-FC and HDL-CE. The HDL-FC:HDL-CE ratio was 1:3 as obtained from Groener et al. (23). This ratio was applied to the HDL-C data above to obtain the HDL-FC and HDL-CE concentration, resulting in 0.30 mM for HDL-FC and 0.89 mM for HDL-CE. No distinction was made between non-HDL-free cholesterol and non-HDL-cholesterol ester (i.e., only the total [non-HDL-C] was considered).

A summary of the results is presented in **Table 3**. Several steady-state reaction rates were not directly obtained from data but instead were calculated from the other reaction rates using mass balances as indicated in Table 3 for v^{ss}_5, v^{ss}_7, v^{ss}_8, v^{ss}_{10-12}, v^{ss}_{17}, and v^{ss}_{19-20}.

The model predicted a steady state that matched all the data in Table 3, which indicates that the data, taken from various sources, were mutually consistent.

Model validation

As a model validation, 10 genetic variations known to affect cholesterol metabolism were simulated, and model predictions for TC, HDL-C, and non-HDL-C were compared with experimental data. The 10 mutations included mutations that cause familial hypercholesterolemia (FH), fish eye disease, Smith-Lemli-Opitz syndrome (SLOS), and other diseases. Details on all 10 mutations (numbered with roman digits) are given in **Table 4** and are explained below. In the list of 10 mutations, two genes were included twice (APOB and LCAT), both as homozygote and as heterozygote variant.

Each mutation was simulated by multiplying the rate constant of the reaction affected with a specific parameter f_{mut} defined for that mutation (see Eq. 15–17; Table 2). The parameter f_{mut} is generally defined as the ratio of the value of a specific variable in carriers of the mutation to the value of that specific variable in controls. The specific affected variables for all mutations are given in Table 4. The parameter f_{mut} for the simulation of a bile acid synthesis defect in the gene CYP7A1 (mutation X), for example, was defined as the ratio of the bile acid contents of the stools from carriers of the mutation to that in controls. The affected individuals had 5% of the amount of bile acids in their stools compared with healthy controls (24). The value of f_{mut} was, therefore, set to 0.05 (Table 4). Values of the parameter f_{mut} range from 0.00 for the SLOS mutation and the homozygote LCAT mutation to 0.65 for a variant of the CETP gene, implying that the list contained mutations that cause both mild and severe phenotypes.

Model predictions and experimental data are given in **Fig. 2** (for TC), **Fig. 3** (HDL-C), and **Fig. 4** (non-HDL-C). Apart from LCAT deficiency (mutation VIII; Table 4), the model correctly predicted whether the TC, HDL-C, and non-HDL-C concentrations were decreased, increased, or relatively unchanged by the mutations. The average relative deviations between model predictions and experimental data were 36%, 49%, and 43% for TC, HDL-C, and non-HDL-C, respectively. This is considered successful within the present state-of-the-art of PBK modeling, where quantitative predictions may generally be correct within one order of magnitude (25–28). These model predictions are generally within the experimental error margin given the small patient groups sizes (generally $n < 20$).

Model analysis

An important step in modeling is model analysis, which is the step in which novel biological insight can be obtained. Model sensitivity analysis was performed to analyze which cholesterol concentrations were most affected by which biological reactions. **Fig. 5** presents the sensitivity coefficients (SC) (Eq. 18) that express the sensitivity of the eight concentrations in the model toward changes in the kinetic parameters of each of the 21 reactions. A positive SC indicates that an increase in the reaction rate constant resulted in an increase of the predicted concentration. A negative SC indicates that an increase in the reaction rate constant resulted in a decrease of the predicted concentration. Some

TABLE 3. Numerical values for the compartmental volumes, steady-state concentrations, and steady-state reaction rates for a 70 kg reference man. The intestinal pools consist of both the cholesterol in lumen and enterocyte. More details can be found in the text and in supplementary material

Organ	Symbol	Value	Obtained from
		Volumes (liters/man)	
Liver	V_{liv}	1.80	Calculated assuming liver mass is 2.57% of total body mass and organ density is 1 kg/l (19).
Intestine	V_{Int}	0.64	Calculated assuming intestinal mass is 0.91% of total body mass and organ density is 1 kg/l (19).
Plasma	V_{Pla}	2.79	Calculated assuming plasma volume is 39.9 ml/kg body mass (51).
Periphery	V_{Per}	64.8	Calculated by subtracting liver, intestinal and plasma mass from the 70 kg total body mass and assuming density is 1 kg/l.
		Steady-state concentrations (mmol per liter tissue or plasma)	
Hepatic free cholesterol	$[C]^{ss}_{Liv\text{-}FC}$	8.00	Measured using needle liver biopsies (52).
HDL free cholesterol	$[C]^{ss}_{HDL\text{-}FC}$	0.30	See text (22,23).
HDL cholesterol ester	$[C]^{ss}_{HDL\text{-}CE}$	0.89	See text (22,23).
Non-HDL cholesterol	$[C]^{ss}_{non\ HDL\text{-}C}$	4.03	See text (22).
Peripheral cholesterol	$[C]^{ss}_{Per\text{-}C}$	1.20	Measured in biopsies from large organs in sudden death individuals (53).
Intestinal free cholesterol	$[C]^{ss}_{Int\text{-}FC}$	1.99	Determined from biopsies from sudden death individuals. (54). Ratio Int-FC:Int-CE was assumed to be equal to that ratio in $CaCO_2$ cells (55).
Intestinal cholesterol ester	$[C]^{ss}_{Int\text{-}CE}$	0.25	Determined from biopsies from sudden death individuals. (54). Ratio Int-FC:Int-CE was assumed to be equal to that ratio in $CaCO_2$ cells (55).
Hepatic cholesterol ester	$[C]^{ss}_{Liv\text{-}CE}$	5.30	Measured using needle liver biopsies (52).
		Steady-state reaction rates (mmol/[man·day])	
Hepatic cholesterol synthesis	v_1^{ss}	0.44	Determined with ex vivo studies on liver biopsies (13,56,57).
Peripheral cholesterol synthesis	v_2^{ss}	3.79	Calculated from total body (determined from squalene kinetics), hepatic, and intestinal cholesterol synthesis rates (56).
Intestinal cholesterol synthesis	v_3^{ss}	0.18	Determined with ex vivo studies on intestinal biopsies (58).
Dietary cholesterol intake	v_4^{ss}	1.09	Calculated using 7 day food recall (59).
Hepatic uptake of cholesterol from non-HDL	v_5^{ss}	11.42	Sum of the uptake rates of non-HDL-C (reactions 5 and reaction 7) was calculated with the LDL-C balance: $v_5^{ss} + v_7^{ss} = v_{21}^{ss} + v_6^{ss} + v_{11}^{ss}$. The ratio between hepatic (v_5^{ss}) and extrahepatic uptake (v_7^{ss}) in the human was assumed to be identical to that ratio in the mouse (60).
Hepatic VLDL-C secretion	v_6^{ss}	4.76	Calculated from stable isotope study (61) and lipoprotein composition data (62).
Peripheral uptake of cholesterol from non-HDL	v_7^{ss}	1.31	See v_5^{ss}.
Peripheral cholesterol transport to HDL	v_8^{ss}	2.48	Calculated with the peripheral cholesterol balance ($v_8^{ss} = v_2^{ss} + v_7^{ss} - v_{12}^{ss}$).
HDL-associated cholesterol esterification	v_9^{ss}	7.86	Determined with ex vivo test with endogenous substrates (63,64).
Hepatic HDL-CE uptake	v_{10}^{ss}	2.93	Calculated with the HDL-CE balance ($v_{10}^{ss} = v_9^{ss} - v_{21}^{ss}$).
Intestinal chylomicron-C secretion	v_{11}^{ss}	3.04	Calculated with the intestinal cholesterol ester balance ($v_{11}^{ss} = v_{20}^{ss}$).
Peripheral cholesterol loss	v_{12}^{ss}	2.62	Calculated with the total body balance $v_{12}^{ss} = v_1^{ss} + v_2^{ss} + v_3^{ss} + v_4^{ss} - v_{18}^{ss} - v_{15}^{ss}$.
Hepatic HDL-FC uptake	v_{13}^{ss}	1.57	Calculated by assuming that the ratio between v_{10} and v_{13} is similar in human and mouse (12).
Biliary cholesterol excretion	v_{14}^{ss}	3.66	Measured using bile that was collected with a swallowed tube (65).
Fecal cholesterol excretion	v_{15}^{ss}	1.85	Measured by fecal collection and analysis (59).
Intestinal cholesterol transport to HDL	v_{16}^{ss}	0.03	Measured using in an in vitro assay with $CaCo_2$ cells (66)
Hepatic cholesterol transport to HDL	v_{17}^{ss}	6.91	Calculated with the hepatic free cholesterol balance ($v_{17}^{ss} = v_1^{ss} + v_{13}^{ss} + v_{10}^{ss} + v_5^{ss} - v_6^{ss} - v_{18}^{ss} - v_{14}^{ss}$).
Hepatic cholesterol catabolism	v_{18}^{ss}	1.03	Assumed to be equal to fecal loss of bile acids, measured by fecal collection and analysis (59).
Hepatic cholesterol esterification	v_{19}^{ss}	4.76	Calculated with the hepatic cholesterol ester balance ($v_{19}^{ss} = v_6^{ss}$).
Intestinal cholesterol esterification	v_{20}^{ss}	3.04	Calculated with the intestinal free cholesterol balance ($v_{20}^{ss} = v_3^{ss} + v_4^{ss} + v_{14}^{ss} - v_{16}^{ss} - v_{15}^{ss}$).
CE transfer from HDL to non-HDL	v_{21}^{ss}	4.93	Measured ex vivo with radiolabeled CE (non-HDL) (21).

concentrations responded to changes in many different rate constants (e.g., hepatic-free cholesterol [Liv-FC]), whereas other concentrations were sensitive to changes in only a few reactions. HDL-FC, for example, was only sensitive ($SC < -0.25$ or $SC > 0.25$) to changes in HDL-associated cholesterol esterification (reaction 9), and hepatic cholesterol transport was only sensitive to HDL (reaction 17; Fig. 5). Fig. 5 indicates that some reactions strongly influenced many concentrations. The rate of hepatic uptake of cholesterol from non-HDL (reaction 5) influenced

JOURNAL OF LIPID RESEARCH ASBMB JLR

TABLE 4. Description of the 10 human mutations used for model validation. The table includes the name of the gene carrying the mutation, the plasma cholesterol levels (TC, HDL-C, and non-HDL-C) of the subjects carrying the mutations (expressed as fold increase relative to the control group), the number of the reaction(s) affected by specific mutations, the severity of the affection expressed as f_{mut} (Eq. 15–17), and the name of the variable used to determine f_{mut}. Reaction numbers correspond to numbers in Fig. 1.

No.	Gene	TC(Relative to Control)	HDL-C (Relative to Control)	non-HDL-C (Relative to Control)	Reaction Affected	f_{mut}	Experimentally Measured Variable Used To Determine f_{mut}	Ref.
I	LDLR[a]	1.85	0.86	2.17	5, 7	0.38	The fractional catabolic rate of APOB in LDL	(61)
II	APOB[b]	1.36	0.85	1.52	5, 7	0.31	The fractional catabolic rate of APOB in LDL	(61)
III	APOB[c]	1.97	1.12	2.24	5, 7	0.32	The fractional catabolic rate of APOB in LDL	(61)
IV	ABCA1[d]	1.07	0.22	1.42	8, 16, 17	0.41	The cholesterol efflux rate to APOA1	(67)
V	APOE[e]	2.80	NA	NA	5, 7	0.45	The residence time of the carrier or control form of APOE in a normal subject	(68)
VI	CETP[f]	1.01	1.10	0.98	21	0.65	The plasma level of CETP	(15)
VII	LCAT[g]	0.81	0.79	0.97	9	0.62	The in vitro determined activity of LCAT	(46)
VIII	LCAT[h]	0.77	0.19	0.82	9	0	The in vitro determined activity of LCAT	(46)
IX	DHCR7[i]	0.20	NA	NA	1, 2, 3	0.00	The cholesterol synthesis activity in cultured fibroblasts	(69,70)
X	CYP7A1[j]	1.74	0.97	2.09	18	0.05	The bile acid content of the stools	(24)

NA, not available
[a] Heterozygote familial hypercholesterolemia (FH).
[b] Heterozygote familial defective APOB (FDB).
[c] Homozygote familial defective APOB (FDB).
[d] Hypoalphalipoproteinemia.
[e] Type III hyperlipoproteinemia.
[f] Heterozygote in exon 15.
[g] Heterozygote familial LCAT deficiency (incl. Fish eye disease).
[h] Homozygote familial LCAT deficiency (incl. Fish eye disease).
[i] Smith-Lemli-Opitz syndrome (SLOS).
[j] Bile acid synthesis defect.

(again |SC| > 0.25) four of the eight pools. In contrast, intestinal cholesterol synthesis (reaction 3) or intestinal cholesterol transport to HDL (reaction 16) did not influence any concentration.

An increased free cholesterol concentration (Liv-FC and Int-FC) is associated with membrane damage and cytotoxicity (29). This model analysis might, therefore, be relevant to predict cytotoxicity: if a reaction highly affects one of these pools, then substances that alter the activity of that reaction may induce cell death.

Fig. 5 shows that Liver FC (Liv-FC) was not only sensitive to changes in the reactions that directly produced or consumed hepatic free cholesterol, such as biliary cholesterol excretion (reactions 14) and hepatic cholesterol catabolism (reaction 18), but also to peripheral cholesterol synthesis (reaction 2) and intestinal cholesterol esterification (reaction 20). Int-FC was primarily sensitive to changes in intestinal cholesterol esterification (reaction 20), biliary cholesterol excretion (reaction 14), and fecal cholesterol secretion (reaction 15).

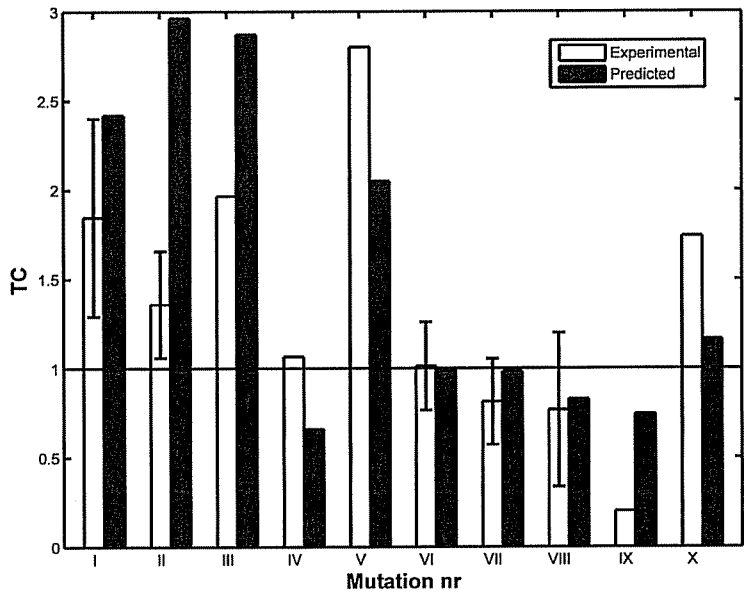

Fig. 2. PBK model predictions compared with experimental data for TC concentrations (relative to control) for 10 different human mutations. Mutation numbers correspond to the numbers in Table 4.

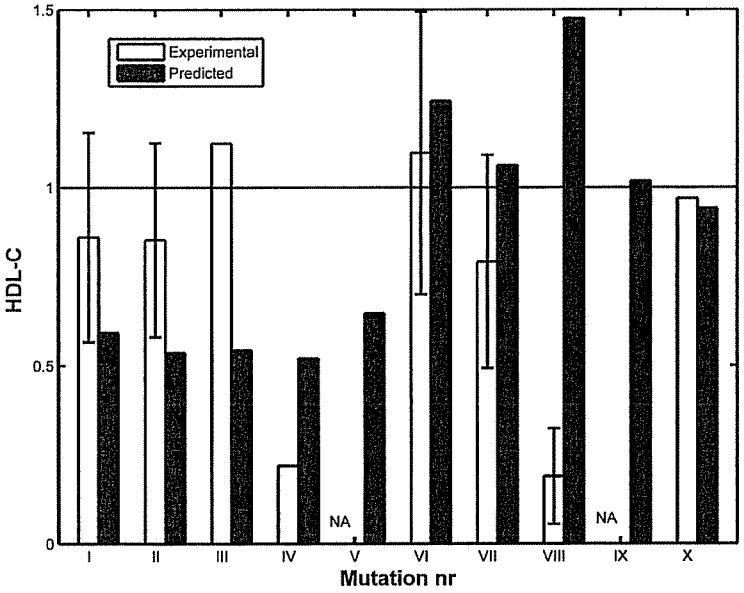

Fig. 3. PBK model predictions compared with experimental data for HDL-C (relative to control) for 10 different human mutations. Mutation numbers correspond to the numbers in Table 4. NA, no data available.

Of special interest for the purpose of the present model are the SC values for cholesterol concentrations in plasma (TC, HDL-C, and non-HDL-C) that are correlated with the risk for coronary heart disease (10). Sensitivity coefficients for the influence of the different reactions on these concentrations are given in **Fig. 6**.

Hepatic uptake of cholesterol from non-HDL (reaction 5), hepatic transport of cholesterol to HDL (reaction 17), and hepatic cholesterol esterification (reaction 19) were the reactions that showed the largest influence on TC (i.e., resulting from the combined influence of these reactions on HDL-C [Fig. 6, middle panel]) and non-HDL-C [Fig. 6, right panel]). Reactions 6, 11, 16, and 21 had the smallest effect on TC. The HDL-C concentration (Fig. 6, middle panel) was mainly dependent on hepatic transport of cholesterol to HDL (reaction 17), CE transfer from HDL to non-HDL (reaction 21), and hepatic uptake of cholesterol from non-HDL (reaction 5). The model predicted (Fig. 6, right panel) that non-HDL-C was highly dependent on hepatic uptake of cholesterol from non-HDL (reaction 5) and mainly on hepatic transport of cholesterol to HDL (reaction 17) and hepatic cholesterol esterification (reaction 19).

In general, as seen in Fig. 6, sensitivity coefficients for TC were more similar to those for non-HDL-C than to those for HDL-C because only a small fraction of plasma cholesterol is present in HDL-C.

Finally, this sensitivity analysis revealed that, according to the model, there are several efficient ways to lower non-HDL-C concentrations and increase HDL-C concentrations simultaneously by modulating only one single reaction (Fig. 6, middle and right panels). The most potent reactions

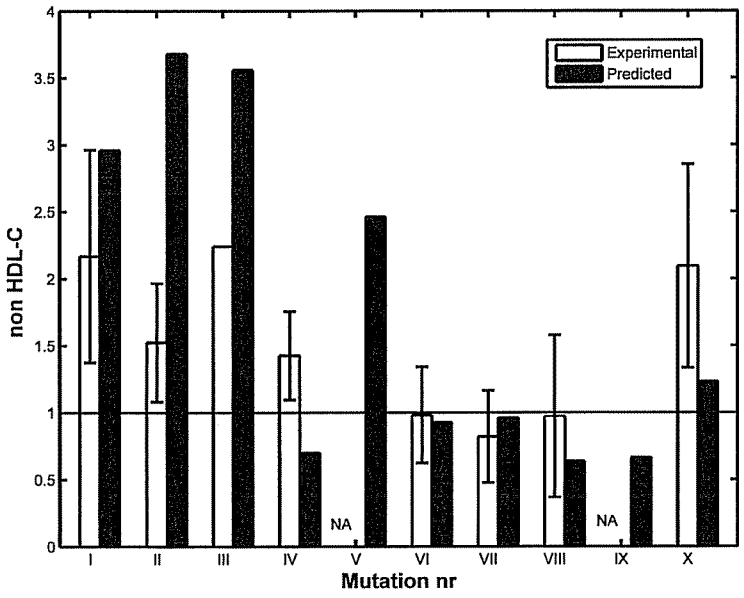

Fig. 4. PBK model predictions compared with experimental data for non-HDL-C (relative to control) for 10 different human mutations. Mutation numbers correspond to the numbers in Table 4. NA, no data available.

ASBMB JOURNAL OF LIPID RESEARCH

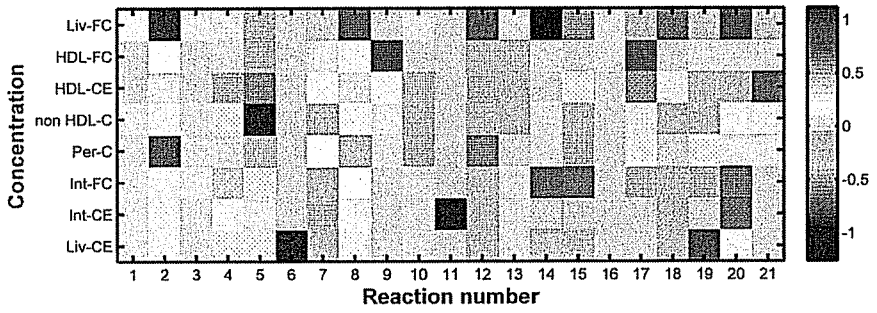

Fig. 5. Color representation of the sensitivity coefficients that quantify the influence of changes in the rate constants of the different reactions on the different concentrations. See text for details. Reaction numbers correspond to the numbers in Figure 1.

seem to be hepatic uptake of non-HDL-C (reaction 5) and CE transfer from HDL to LDL (reaction 21). The first reaction is targeted indirectly by statins (30). The latter reaction is targeted by CETP inhibitors, a drug class of which several members (e.g., dalcetrapib) were recently tested in clinical trials (16, 31, 32).

DISCUSSION

In silico models have been used for various purposes in the study of cholesterol metabolism, such as in the interpretation of isotope-labeling studies (4–6, 33), in the analysis of the regulatory pathway of cholesterol synthesis (34), or in making predictions of the effect of genetic mutations or food and drug interventions (35, 36). These models, however, could predict the effect of a few genetic mutations only. The aim of this study was to develop a model that can be applied in the prediction of a wide variety of genetic, nutritional, and pharmaceutical effects on plasma cholesterol levels.

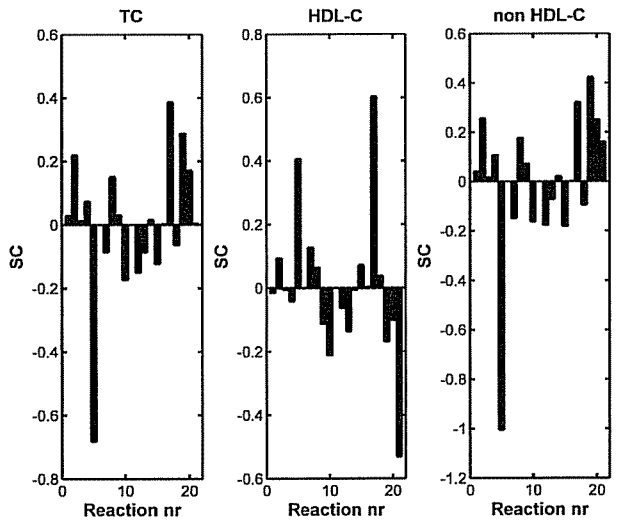

Fig. 6. Sensitivity coefficients (see Eq. 18) for the different reactions toward TC (left panel), HDL-C (middle panel), and non-HDL-C (right panel). Reaction numbers correspond to the numbers in Figure 1.

As all models, our model is a compromise between simplicity and complexity (37). A too simple model is not useful to simulate multiple interventions because such a model will lack the targets of at least part of these interventions. A too complex model is not useful either because insufficient experimental data will be present to define the parameters (calibration) or to validate the model.

One of the important necessary simplifications made was to restrict the description of lipoprotein metabolism to cholesterol alone. As a consequence, no distinction was made between different fractions of non-HDL-C (i.e., LDL, IDL, and VLDL) in the present model. Including a more detailed mechanistic description of lipoprotein metabolism is a highly complex task that will necessitate to, for example, include the link between cholesterol metabolism and triglyceride metabolism. Although significant progress in this field is being made (4, 38, 39), this was considered too ambitious for the present stage of model development.

As a consequence of these necessary simplifications, rates derived from model-based interpretation of stable isotope tracer data were unsuited for model calibration because the structure of well-established isotopic tracer kinetic models (33 and references therein) did not match with the present model due to different aggregations of reactions. A factor further hampering the use of these data is that the tracer analysis considers bidirectionality of fluxes, whereas our PBK model formulation had to be limited to unidirectional (i.e., net) fluxes to keep the number of parameters at a minimum. As a result, using the isotopic flux data for calibration of the PBK model was not possible.

The following two examples illustrate some of the difficulties arising from the different structures of the present PBK model vs. the established tracer kinetic models described in Schwartz et al. (33): (*1*) The tracer kinetic model assumes all cholesterol to be synthesized in the liver, whereas in the present PBK model the liver contributed only 10% of total cholesterol synthesis, in line with data from Dietschy and Turley (40). (*2*) Schwartz et al. (33) reported that the liver does not take up HDL-CE, whereas the corresponding reaction (reaction 10) in the PBK model carries a considerable flux (2.93 mmol/man/day),

which is more in line with the statement of Rinninger et al. (41) based on data obtained with primary hepatocytes (i.e., "high-density lipoprotein cholesteryl esters were selectively taken up by hepatocytes and are hydrolyzed independently from the classical lysosomal catabolic pathway"). Thus, although the two models differ markedly in structure, supporting evidence for the PBK model structure can also be found in the literature. This suggest that valuable insights could be obtained from future work that would analyze structure variations in both models while taking calibration data for both models into account. For instance, one could investigate whether directing v_5 and v_{10} into liver CE and adding a pathway that is the reverse of v_{19} to represent lysosomal hydrolases is equivalent (in terms of outcomes and conclusions) to directing them into the liver FC pool as in the present PBK model. Likewise, different alternative structures of the tracer kinetic models may be investigated that are more in line with the PBK model. Such models could, for example, incorporate constraints on net fluxes derived from the PBK model in the isotopic tracer data analysis.

The level of complexity of the model described here was apparently an acceptable compromise because the model could successfully be calibrated from literature data by flux balancing with only a limited set of assumptions (see supplementary information). Nevertheless, the consequences of the implemented calibration procedure may be a point for further attention. Data used were from a variety of different unconnected studies that used different experimental protocols and methods, often applied to very small groups of subjects of different weight and age. This carries the inherent risk of data inconsistencies and potentially large influences of individual variation. Although this risk was mitigated as much as possible by scaling all data to a 70 kg reference man, questions may remain as to the impact of the calibration on the predictions by the model. The sensitivity analysis gives some insight in this issue (i.e., from Fig. 6 it appears that variation of reactions 6, 11, and 16 will have little influence on the plasma cholesterol predictions of the model). Although a full variability analysis would be required to cover this issue, this was not feasible because data are too sparse to give a statistically meaningful estimate and to validate the analysis, but we generally saw a 25% variation across any dataset. Rather, we discuss in the following sections some specific results that seem at variance with established cholesterol flux analysis literature (33 and references therein). Peripheral cholesterol loss (reaction 12) was 2.62 mmol/man/day, which is comparable to the sum of net bile acid loss (1.03 mmol/man/day) and net fecal cholesterol loss (1.85 mmol/man/day), which are generally considered the main routes for cholesterol loss from the body. Beyond skin sloughing and steroid hormone production, one could ask which candidate processes could carry this flux. Because the estimation of total cholesterol synthesis is based on in vivo squalene isotopic labeling data, we do not consider a mistake in this estimation as a possible explanation for the missing peripheral cholesterol excretion. Rather, we hypothesize that sebum production might contribute considerably in this regard. Human sebum secretion rates from forehead skin are reported to lie between 1.3 and 3.3 mg/10 cm^2/3 h (42). NMR studies indicate that the molar fractions of CE and squalene in sebum are 0.03 and 0.28, respectively, with the other constituents being triglycerides, fatty acids, and wax esters (43). With a total body area of approximately 2 m^2, taking into account the molar weights of the different constituents and assuming uniform secretion rates, an upper bound for the total CE and squalene flux may be as high as 2.5 mmol/man/day. Although this estimation seems to support the possibility that peripheral cholesterol loss may be as high as the model calibration suggests, independent validation experiments are necessary to confirm the hypothesis that sebum excretion is a possible explanation for the missing peripheral cholesterol excretion.

Another item is the transfer of FC from liver to HDL (v_{17}, 6.91 mmol/man/day), which in the present analysis greatly exceeded total hepatic uptake of HDL-FC and HDL-CE combined (v_{10} + v_{13}, 4.50 mmol/man/day), whereas in Schwartz et al. (33) the reverse was observed (i.e., more liver uptake of HDL-C than transfer from liver to HDL). However, in Schwartz et al. (33), this net flux is the difference between very high fluxes (> 46 mmol/man/day) that operate in both directions. Thus, both models indicate a large contribution to plasma HDL coming from the liver. This has also been observed in animal studies and in our previous mouse work (12).

These observations indicate that, although the flux distribution in our model deviated strongly from that seen in established isotope tracer studies for reasons discussed above, supporting evidence for the PBK model structure and flux predictions can be found in the literature.

The key question is whether the model is valid for its intended use to predict changes in plasma cholesterol concentrations following different dietary regimens, pharmacological treatments, or genetic variation. Indeed, the PBK model was able to predict the effects of 10 human mutations (Figs. 2–4), including a mutation in the LDLR gene (mutation I, responsible for FH) and the DHCR7 gene (mutations IX, responsible for SLOS). While simulating this latter syndrome, negative concentrations were predicted for several submodels. This must be due to the fact that these submodels retain zero-order kinetics (i.e., saturated Michaelis-Menten kinetics) when under the extreme conditions associated with blocked cholesterol synthesis in SLOS (44), cholesterol concentrations are lowered to such an extent that first-order kinetics would be more appropriate.

Model predictions for TC deviated on average less than 40% from experimentally observed values, which is relatively good compared with the current state of the art for PBK models of exogenous substances (26–28, 45). This is all the more remarkable because the model was obtained via a relatively straightforward translational adaptation of our previously developed mouse model.

The only case where a large deviation between model predictions and experimental data (HDL-C concentration) were seen is in LCAT deficiency: mutation VIII. The model

predicted an increase in HDL-C, whereas a decrease is observed in reality (Fig. 3). This increase is in the form of HDL-FC and not in HDL-CE (data not shown). The resulting shift in CE/FC ratio predicted by the model is in fact similar, as seen in the literature (46). A possible explanation for the deviation between model predictions and experimental data is that, in reality, a maximum of HDL-FC might exist. If this maximum is reached, the transport of free cholesterol to HDL (reactions 8, 16, and 17) will be inhibited, thereby causing HDL-C lowering. The model in its present form does not take this into account.

As shown in Fig. 6, the model predicted that an increased dietary intake of cholesterol (reaction 4) will lead to an increased TC level, an increased non-HDL-C level, and a slightly lowered HDL-C level. This is in agreement with findings in nutritional studies (see meta-analysis in Ref. 47). The model also predicted that non-HDL-C is mostly affected by hepatic cholesterol esterification (reaction 19) and hepatic uptake of cholesterol from LDL (reaction 5). This confirms that the liver is a dominant organ in determining the plasma cholesterol levels (13).

A decrease in hepatic cholesterol synthesis (reaction 1) resulted in a decrease of the non-HDL-C (Fig. 6, right panel) and in an increase of HDL-C. This is in agreement with the outcome of statin-mediated inhibition of hepatic cholesterol synthesis (48). In reality, statin therapy will also cause an up-regulation of the LDLR and thereby the activity of hepatic non-HDL-C uptake, increasing the non-HDL-C lowering effect.

A decrease in the activity of CETP (reaction 21) had a larger relative effect on HDL-C than on non-HDL-C (Fig. 6). This is in agreement with the outcome of torcetrapib-mediated CETP inhibition (49) and CETP mutations (mutation VI, Table 4). Taken together, these findings illustrate that the described model can indeed be helpful to predict effects of dietary and pharmaceutical interventions.

A recent genome-wide association study (GWAS) has found 95 SNPs that correlated with altered TC, HDL-C, LDL-C, or triglycerides concentrations (50). At least 19 of these SNPs were near genes that are involved in one or more of the reactions in the model. The gene ABCA1, for example, is involved in the transport of cholesterol to HDL (reactions 8, 16, and 17).

We compared effect sizes of the 19 SNPs given by Teslovich et al. (50) with the sensitivity coefficients of associated reactions (Fig. 6) by Spearman correlation and found a positive correlation between our findings and the ones reported by Teslovich et al. (50) for HDL-C, LDL-C, and TC (all $P < 0.05$) (data not shown). This is an additional validation of the present model and implies that the developed model is useful to study the implications of genetic variations on cholesterol metabolism.

The GWAS study (50) also reports several SNPs correlating with cholesterol concentrations in plasma near genes that could not be directly linked to a specific reaction in our model (Fig. 1), like in HNF4A, CILP2, and ANGPTL3. This absence of a direct link is the result of essential simplifications needed to construct the model.

We conclude that the approach of first developing a computational PBK model for the mouse and then translating it into a human model as described in this paper resulted in an accurate model for the prediction of plasma cholesterol concentrations in humans. Sensitivity coefficients derived from the model correlated well with recent independent GWAS data on plasma cholesterol. Because the model correctly predicted key features of the effect of increased dietary cholesterol intake and of statin treatment and CETP inhibition, we expect that the model can also be used to predict the effects of a wider variety of pharmacological and dietary interventions on plasma cholesterol levels in humans, which will be the subject of further work.

REFERENCES

1. Fell, D. 1997. Understanding the control of metabolism. Portland Press, London, UK.
2. Rietjens, I. M., M. G. Boersma, M. Zaleska, and A. Punt. 2008. Differences in simulated liver concentrations of toxic coumarin metabolites in rats and different human populations evaluated through physiologically based biokinetic (PBBK) modeling. *Toxicol. In Vitro.* **22:** 1890–1901.
3. Reddy, M. B., R. S. H. Yang, H. J. Clewell, and M. E. Andersen. 2005. Physiologically based pharmacokinetic modeling. John Wiley & Sons, Inc., Hoboken, NJ.
4. van Schalkwijk, D. B., A. A. de Graaf, B. van Ommen, K. van Bochove, P. C. Rensen, L. M. Havekes, N. C. van de Pas, H. C. Hoefsloot, J. van der Greef, and A. P. Freidig. 2009. Improved cholesterol phenotype analysis by a model relating lipoprotein life cycle processes to particle size. *J. Lipid Res.* **50:** 2398–2411.
5. Adiels, M., C. Packard, M. J. Caslake, P. Stewart, A. Soro, J. Westerbacka, B. Wennberg, S. O. Olofsson, M. R. Taskinen, and J. Boren. 2005. A new combined multicompartmental model for apolipoprotein B-100 and triglyceride metabolism in VLDL subfractions. *J. Lipid Res.* **46:** 58–67.
6. Packard, C. J., and J. Shepherd. 1997. Lipoprotein heterogeneity and apolipoprotein B metabolism. *Arterioscler. Thromb. Vasc. Biol.* **17:** 3542–3556.
7. Ratushnyi, A. V., V. A. Likhoshvai, E. V. Ignat'eva, Y. G. Matushkin, I. I. Goryanin, and N. A. Kolchanov. 2003. A computer model of the gene network of the cholesterol biosynthesis regulation in the cell: analysis of the effect of mutations. *Dokl. Biochem. Biophys.* **389:** 90–93.
8. Rosamond, W., K. Flegal, K. Furie, A. Go, K. Greenlund, N. Haase, S. M. Hailpern, M. Ho, V. Howard, B. Kissela, et al. 2008. Heart disease and stroke statistics–2008 update: a report from the American Heart Association Statistics Committee and Stroke Statistics Subcommittee. *Circulation.* **117:** e25–e146.
9. Glassberg, H., and D. J. Rader. 2008. Management of lipids in the prevention of cardiovascular events. *Annu. Rev. Med.* **59:** 79–94.
10. Lusis, A. J. 2000. Atherosclerosis. *Nature.* **407:** 233–241.
11. van de Pas, N. C., A. E. Soffers, A. P. Freidig, B. van Ommen, R. A. Woutersen, I. M. Rietjens, and A. A. de Graaf. 2010. Systematic construction of a conceptual minimal model of plasma cholesterol levels based on knockout mouse phenotypes. *Biochim. Biophys. Acta.* **1801:** 646–654.
12. van de Pas, N. C., R. A. Woutersen, B. van Ommen, I. M. Rietjens, and A. A. de Graaf. 2011. A physiologically-based kinetic model for the prediction of plasma cholesterol concentrations in the mouse. *Biochim. Biophys. Acta.* **1811:** 333–342.
13. Dietschy, J. M., and S. D. Turley. 2002. Control of cholesterol turnover in the mouse. *J. Biol. Chem.* **277:** 3801–3804.
14. Agellon, L. B., A. Walsh, T. Hayek, P. Moulin, X. C. Jiang, S. A. Shelanski, J. L. Breslow, and A. R. Tall. 1991. Reduced high density lipoprotein cholesterol in human cholesteryl ester transfer protein transgenic mice. *J. Biol. Chem.* **266:** 10796–10801.
15. Zhong, S., D. S. Sharp, J. S. Grove, C. Bruce, K. Yano, J. D. Curb, and A. R. Tall. 1996. Increased coronary heart disease in Japanese-American men with mutation in the cholesteryl ester transfer protein gene despite increased HDL levels. *J. Clin. Invest.* **97:** 2917–2923.

16. Barter, P. J., M. Caulfield, M. Eriksson, S. M. Grundy, J. J. Kastelein, M. Komajda, J. Lopez-Sendon, L. Mosca, J. C. Tardif, D. D. Waters, et al. 2007. Effects of torcetrapib in patients at high risk for coronary events. *N. Engl. J. Med.* **357:** 2109–2122.
17. Clark, R. W., T. A. Sutfin, R. B. Ruggeri, A. T. Willauer, E. D. Sugarman, G. Magnus-Aryitey, P. G. Cosgrove, T. M. Sand, R. T. Wester, J. A. Williams, et al. 2004. Raising high-density lipoprotein in humans through inhibition of cholesteryl ester transfer protein: an initial multidose study of torcetrapib. *Arterioscler. Thromb. Vasc. Biol.* **24:** 490–497.
18. Davidson, M. H., J. M. McKenney, C. L. Shear, and J. H. Revkin. 2006. Efficacy and safety of torcetrapib, a novel cholesteryl ester transfer protein inhibitor, in individuals with below-average high-density lipoprotein cholesterol levels. *J. Am. Coll. Cardiol.* **48:** 1774–1781.
19. Brown, R. P., M. D. Delp, S. L. Lindstedt, L. R. Rhomberg, and R. P. Beliles. 1997. Physiological parameter values for physiologically based pharmacokinetic models. *Toxicol. Ind. Health.* **13:** 407–484.
20. Potter, L. K., D. L. Sprecher, M. C. Walker, and F. L. Tobin. 2009. Mechanism of inhibition defines CETP activity: a mathematical model for CETP in vitro. *J. Lipid Res.* **50:** 2222–2234.
21. Morton, R. E., and D. J. Greene. 2003. The surface cholesteryl ester content of donor and acceptor particles regulates CETP: a liposome-based approach to assess the substrate properties of lipoproteins. *J. Lipid Res.* **44:** 1364–1372.
22. Carroll, M. D., D. A. Lacher, P. D. Sorlie, J. I. Cleeman, D. J. Gordon, M. Wolz, S. M. Grundy, and C. L. Johnson. 2005. Trends in serum lipids and lipoproteins of adults, 1960–2002. *JAMA.* **294:** 1773–1781.
23. Groener, J. E., L. M. Scheek, E. van Ramshorst, X. H. Krauss, and A. van Tol. 1998. Delayed increase in high density lipoprotein-phospholipids after ingestion of a fat load in normolipidemic patients with coronary artery disease. *Atherosclerosis.* **137:** 311–319.
24. Pullinger, C. R., C. Eng, G. Salen, S. Shefer, A. K. Batta, S. K. Erickson, A. Verhagen, C. R. Rivera, S. J. Mulvihill, M. J. Malloy, et al. 2002. Human cholesterol 7alpha-hydroxylase (CYP7A1) deficiency has a hypercholesterolemic phenotype. *J. Clin. Invest.* **110:** 109–117.
25. Punt, A., A. Paini, M. G. Boersma, A. P. Freidig, T. Delatour, G. Scholz, B. Schilter, P. J. van Bladeren, and I. M. Rietjens. 2009. Use of physiologically based biokinetic (PBBK) modeling to study estragole bioactivation and detoxification in humans as compared with male rats. *Toxicol. Sci.* **110:** 255–269.
26. Lupfert, C., and A. Reichel. 2005. Development and application of physiologically based pharmacokinetic-modeling tools to support drug discovery. *Chem. Biodivers.* **2:** 1462–1486.
27. Hissink, A. M., B. van Ommen, J. Kruse, and P. J. van Bladeren. 1997. A physiologically based pharmacokinetic (PB-PK) model for 1,2-dichlorobenzene linked to two possible parameters of toxicity. *Toxicol. Appl. Pharmacol.* **145:** 301–310.
28. Quick, D. J., and M. L. Shuler. 1999. Use of in vitro data for construction of a physiologically based pharmacokinetic model for naphthalene in rats and mice to probe species differences. *Biotechnol. Prog.* **15:** 540–555.
29. Tabas, I. 1997. Free cholesterol-induced cytotoxicity. *Trends Cardiovasc. Med.* **7:** 256–263.
30. Davidson, M. H., and P. P. Toth. 2004. Comparative effects of lipid-lowering therapies. *Prog. Cardiovasc. Dis.* **47:** 73–104.
31. de Grooth, G. J., J. A. Kuivenhoven, A. F. Stalenhoef, J. de Graaf, A. H. Zwinderman, J. L. Posma, A. van Tol, and J. J. Kastelein. 2002. Efficacy and safety of a novel cholesteryl ester transfer protein inhibitor, JTT-705, in humans: a randomized phase II dose-response study. *Circulation.* **105:** 2159–2165.
32. Katsnelson, A. 2010. Good news for 'good' cholesterol. *Nature.* **468:** 354.
33. Schwartz, C. C., J. M. VandenBroek, and P. S. Cooper. 2004. Lipoprotein cholesteryl ester production, transfer, and output in vivo in humans. *J. Lipid Res.* **45:** 1594–1607.
34. Kervizic, G., and L. Corcos. 2008. Dynamical modeling of the cholesterol regulatory pathway with Boolean networks. *BMC Syst. Biol.* **2:** 99.
35. Knoblauch, H., H. Schuster, F. C. Luft, and J. Reich. 2000. A pathway model of lipid metabolism to predict the effect of genetic variability on lipid levels. *J. Mol. Med.* **78:** 507–515.
36. Muzaffer Demirezen, E. 2009. A simulation model for blood cholesterol dynamics and related disorders. M.S. thesis. Graduate Program in Industrial Engineering, Bogazici University, Istanbul, Turkey.
37. Ostlund, R. E., Jr. 1993. A minimal model for human whole body cholesterol metabolism. *Am. J. Physiol.* **265:** E513–E520.
38. Hubner, K., T. Schwager, K. Winkler, J. G. Reich, and H. G. Holzhutter. 2008. Computational lipidology: predicting lipoprotein density profiles in human blood plasma. *PLOS Comput. Biol.* **4:** e1000079.
39. Tiemann, C. A., J. Vanlier, P. A. J. Hilbers, and N. A. W. van Riel. 2011. Parameter adaptations during phenotype transitions in progressive diseases. *BMC Syst. Biol.* **5:** 174–187.
40. Dietschy, J. M., and S. D. Turley. 2004. Cholesterol metabolism in the central nervous system during early development and in the mature animal. *J. Lipid Res.* **45:** 1375–1397.
41. Rinninger, F., S. Jaeckle, and R. C. Pittman. 1993. A pool of reversibly cell-associated cholesteryl esters involved in the selective uptake of cholesteryl esters from high-density lipoproteins by Hep G2 hepatoma cells. *Biochim. Biophys. Acta.* **1166:** 275–283.
42. Tayfun Güldür, T., N. Bayraktar, Ö. Kaynar, G. Beker, M. Koçer, and H. Özcan. 2007. Excretion rate and composition of skin surface lipids on the foreheads of adult males with type IV hyperlipoproteinemia. *J. Basic Clin. Physiol. Pharmacol.* 18: 21–35.
43. Robosky, L. C., K. Wade, D. Woolson, J. D. Baker, M. L. Manning, D. A. Gage, and M. D. Reily. 2008. Quantitative evaluation of sebum lipid components with nuclear magnetic resonance. *J. Lipid Res.* **49:** 686–692.
44. Waterham, H. R., F. A. Wijburg, R. C. Hennekam, P. Vreken, B. T. Poll-The, L. Dorland, M. Duran, P. E. Jira, J. A. Smeitink, R. A. Wevers, et al. 1998. Smith-Lemli-Opitz syndrome is caused by mutations in the 7-dehydrocholesterol reductase gene. *Am. J. Hum. Genet.* **63:** 329–338.
45. Punt, A., A. P. Freidig, T. Delatour, G. Scholz, M. G. Boersma, B. Schilter, P. J. van Bladeren, and I. M. Rietjens. 2008. A physiologically based biokinetic (PBBK) model for estragole bioactivation and detoxification in rat. *Toxicol. Appl. Pharmacol.* **231:** 248–259.
46. Calabresi, L., L. Pisciotta, A. Costantin, I. Frigerio, I. Eberini, P. Alessandrini, M. Arca, G. B. Bon, G. Boscutti, G. Busnach, et al. 2005. The molecular basis of lecithin:cholesterol acyltransferase deficiency syndromes: a comprehensive study of molecular and biochemical findings in 13 unrelated Italian families. *Arterioscler. Thromb. Vasc. Biol.* **25:** 1972–1978.
47. Clarke, R., C. Frost, R. Collins, P. Appleby, and R. Peto. 1997. Dietary lipids and blood cholesterol: quantitative meta-analysis of metabolic ward studies. *BMJ.* **314:** 112–117.
48. Nicholls, S. J., E. M. Tuzcu, I. Sipahi, A. W. Grasso, P. Schoenhagen, T. Hu, K. Wolski, T. Crowe, M. Y. Desai, S. L. Hazen, et al. 2007. Statins, high-density lipoprotein cholesterol, and regression of coronary atherosclerosis. *JAMA.* **297:** 499–508.
49. Kastelein, J. J., S. I. van Leuven, L. Burgess, G. W. Evans, J. A. Kuivenhoven, P. J. Barter, J. H. Revkin, D. E. Grobbee, W. A. Riley, C. L. Shear, et al. 2007. Effect of torcetrapib on carotid atherosclerosis in familial hypercholesterolemia. *N. Engl. J. Med.* **356:** 1620–1630.
50. Teslovich, T. M., K. Musunuru, A. V. Smith, A. C. Edmondson, I. M. Stylianou, M. Koseki, J. P. Pirruccello, S. Ripatti, D. I. Chasman, C. J. Willer, et al.: 2010. Biological, clinical and population relevance of 95 loci for blood lipids. *Nature.* **466:** 707–713.
51. Retzlaff, J. A., W. N. Tauxe, J. M. Kiely, and C. F. Stroebel. 1969. Erythrocyte volume, plasma volume, and lean body mass in adult men and women. *Blood.* **33:** 649–661.
52. Honda, A., T. Yoshida, N. Tanaka, Y. Matsuzaki, B. He, J. Shoda, and T. Osuga. 1995. Accumulation of 7 alpha-hydroxycholesterol in liver tissue of patients with cholesterol gallstones. *J. Gastroenterol.* **30:** 651–656.
53. Crouse, J. R., S. M. Grundy, and E. H. Ahrens, Jr. 1972. Cholesterol distribution in the bulk tissues of man: variation with age. *J. Clin. Invest.* **51:** 1292–1296.
54. Chobanian, A. V., and W. Hollander. 1965. Tissue distribution of cholesterol and 24-dehydrocholesterol during chronic triparanol therapy. *J. Lipid Res.* **6:** 37–42.
55. Ranheim, T., B. Halvorsen, A. C. Huggett, R. Blomhoff, and C. A. Drevon. 1995. Effect of a coffee lipid (cafestol) on regulation of lipid metabolism in CaCo-2 cells. *J. Lipid Res.* **36:** 2079–2089.
56. McNamara, D. J., E. H. Ahrens, Jr., P. Samuel, and J. R. Crouse. 1977. Measurement of daily cholesterol synthesis rates in man by assay of the fractional conversion of mevalonic acid to cholesterol. *Proc. Natl. Acad. Sci. USA.* **74:** 3043–3046.
57. Dietschy, J. M., S. D. Turley, and D. K. Spady. 1993. Role of liver in the maintenance of cholesterol and low density lipoprotein homeostasis in different animal species, including humans. *J. Lipid Res.* **34:** 1637–1659.

58. Dietschy, J. M., and W. G. Gamel. 1971. Cholesterol synthesis in the intestine of man: regional differences and control mechanisms. *J. Clin. Invest.* **50:** 872–880.
59. Miettinen, T. A., and Y. A. Kesaniemi. 1989. Cholesterol absorption: regulation of cholesterol synthesis and elimination and within-population variations of serum cholesterol levels. *Am. J. Clin. Nutr.* **49:** 629–635.
60. Xie, C., S. D. Turley, and J. M. Dietschy. 2009. ABCA1 plays no role in the centripetal movement of cholesterol from peripheral tissues to the liver and intestine in the mouse. *J. Lipid Res.* **50:** 1316–1329.
61. Gaffney, D., L. Forster, M. J. Caslake, D. Bedford, J. P. Stewart, G. Stewart, G. Wieringa, M. Dominiczak, J. P. Miller, and C. J. Packard. 2002. Comparison of apolipoprotein B metabolism in familial defective apolipoprotein B and heterogeneous familial hypercholesterolemia. *Atherosclerosis.* **162:** 33–43.
62. Gylling, H., and T. A. Miettinen. 1992. Cholesterol absorption and synthesis related to low density lipoprotein metabolism during varying cholesterol intake in men with different apoE phenotypes. *J. Lipid Res.* **33:** 1361–1371.
63. Funke, H., A. von Eckardstein, P. H. Pritchard, J. J. Albers, J. J. Kastelein, C. Droste, and G. Assmann. 1991. A molecular defect causing fish eye disease: an amino acid exchange in lecithin-cholesterol acyltransferase (LCAT) leads to the selective loss of alpha-LCAT activity. *Proc. Natl. Acad. Sci. USA.* **88:** 4855–4859.
64. Funke, H., A. von Eckardstein, P. H. Pritchard, M. Karas, J. J. Albers, and G. Assmann. 1991. A frameshift mutation in the human apolipoprotein A-I gene causes high density lipoprotein deficiency, partial lecithin: cholesterol-acyltransferase deficiency, and corneal opacities. *J. Clin. Invest.* **87:** 371–376.
65. Bennion, L. J., and S. M. Grundy. 1975. Effects of obesity and caloric intake on biliary lipid metabolism in man. *J. Clin. Invest.* **56:** 996–1011.
66. Field, F. J., K. Watt, and S. N. Mathur. 2008. Origins of intestinal ABCA1-mediated HDL-cholesterol. *J. Lipid Res.* **49:** 2605–2619.
67. Mott, S., L. Yu, M. Marcil, B. Boucher, C. Rondeau, and J. Genest, Jr. 2000. Decreased cellular cholesterol efflux is a common cause of familial hypoalphalipoproteinemia: role of the ABCA1 gene mutations. *Atherosclerosis.* **152:** 457–468.
68. Gregg, R. E., L. A. Zech, E. J. Schaefer, and H. B. Brewer, Jr. 1981. Type III hyperlipoproteinemia: defective metabolism of an abnormal apolipoprotein E. *Science.* **211:** 584–586.
69. Jira, P. E., J. G. de Jong, F. S. Janssen-Zijlstra, U. Wendel, and R. A. Wevers. 1997. Pitfalls in measuring plasma cholesterol in the Smith-Lemli-Opitz syndrome. *Clin. Chem.* **43:** 129–133.
70. Wanders, R. J., G. J. Romeijn, F. Wijburg, R. C. Hennekam, J. de Jong, R. A. Wevers, and G. Dacremont. 1997. Smith-Lemli-Opitz syndrome: deficient delta 7-reductase activity in cultured skin fibroblasts and chorionic villus fibroblasts and its application to pre- and postnatal detection. *J. Inherit. Metab. Dis.* **20:** 432–436.